

To appear in ApJL

Mid-Infrared Diagnostics of LINERs

E. Sturm,¹ D. Rupke,² A. Contursi,¹ D.-C. Kim,² D. Lutz,¹ H. Netzer,^{1,3} S. Veilleux,² R. Genzel,¹ M. Lehnert,¹ L. J. Tacconi,¹ D. Maoz,³ J. Mazzarella,⁴ S. Lord,⁴ D. Sanders,⁵ A. Sternberg³

ABSTRACT

We report results from the first mid-infrared spectroscopic study of a comprehensive sample of 33 LINERs, observed with the *Spitzer Space Telescope*. We compare the properties of two different LINER populations: infrared-faint LINERs, with LINER emission arising mostly in compact nuclear regions, and infrared-luminous LINERs, which often show spatially extended (non-AGN) LINER emission. We show that these two populations can be easily distinguished by their mid-infrared spectra in three different ways: (i) their mid-IR spectral energy distributions (SEDs), (ii) the emission features of polycyclic aromatic hydrocarbons (PAHs), and (iii) various combinations of IR fine-structure line ratios. IR-luminous LINERs show mid-IR SEDs typical of starburst galaxies, while the mid-IR SEDs of IR-faint LINERs are much bluer. PAH flux ratios are significantly different in the two groups. Fine structure emission lines from highly excited gas, such as [OIV], are detected in both populations, suggesting the presence of an additional AGN also in a large fraction of IR-bright LINERs, which contributes little to the combined mid-IR light. The two LINER groups occupy different regions of mid-infrared emission-line excitation diagrams. The positions of the various LINER types in our diagnostic diagrams provide important clues regarding the power source of each LINER type. Most of these mid-infrared diagnostics can be applied at low spectral resolution, making AGN- and starburst-excited LINERs distinguishable also at high redshifts.

¹Max-Planck-Institut für extraterrestrische Physik, Postfach 1312, D-85741 Garching, Germany; sturm@mpe.mpg.de

²Department of Astronomy, University of Maryland, College Park, MD 20742, USA

³School of Physics and Astronomy, Tel Aviv University, Ramat Aviv, Tel Aviv 69978, Israel

⁴IPAC/Caltech, MS 100-22, Pasadena, CA 91125, USA

⁵Institute for Astronomy, University, of Hawaii, 2680 Woodlawn Drive, Honolulu, HI 96822, USA

Subject headings: infrared: galaxies — galaxies: active

1. Introduction

Since their identification as a class of galactic nuclei more than 25 years ago (Heckman 1980), the nature of Low-Ionization Nuclear Emission-Line Regions (LINERs) has remained controversial. Their optical spectra are characterized by enhanced narrow emission lines of low ionization species, quite distinct from those of both H II regions and classical active galactic nuclei (AGNs). They are found in one third to one half of nearby galaxies of all types (e.g., Ho, Filippenko, & Sargent 1997). In many LINERs the emission is concentrated near the nucleus (a few 100 pc, e.g. Pogge et al. 2000) but in others it extends over larger regions, up to a few kpc (Veilleux et al. 1995). There is substantial evidence that many LINERs are powered by accretion onto massive black holes, and that these objects, due to low accretion rates, constitute the low-luminosity end of the AGN class (Quataert 2001, Kewley et al. 2006). If many LINERs at low and high redshifts are indeed low-luminosity AGNs, this would have a significant impact on major issues in astronomy such as the growth history of central black holes and the relation of AGNs to galaxy formation and evolution.

Alternative scenarios for LINER excitation mechanisms have been suggested. Models focusing on photoionization by the central AGN continuum (e.g., Ferland and Netzer 1983; Groves et al. 2004), have been complemented by stellar photoionization modeling (e.g., Barth and Shields 2000) and observations (e.g., Maoz et al. 1998) showing that, under certain conditions, a young starburst can also excite a LINER. In many cases LINER-like emission is also observed on larger spatial scales; these ‘extended’ LINERs tend to be associated with high infrared luminosity (see §2). In addition to nuclear (Black Hole or stellar) photoionization, these sources can be ionized by shock heating through cloud collisions induced by accretion, galaxy interactions, mergers, or starburst-driven winds (e.g. Shull & McKee 1979; Veilleux & Osterbrock 1987; Dopita & Sutherland 1995).

Determining which LINERs are photoionized by a hard, nuclear power source and which are excited by other ionization processes is crucial for understanding not only the local LINER population, but also AGNs and starbursts at high redshifts, if the fraction of LINERs among high- z galaxies is as high as in the local universe. Galaxies with high infrared luminosities and galaxy interactions are much more common at high redshifts than at $z \approx 0$ (e.g. Pérez-González et al. 2005). Whether or not these galaxies host dominant AGNs is an open question. X-ray and radio observations help to identify AGNs in the nuclei of these galaxies. However, they may face problems in deriving the *relative contributions* of AGN and starbursts to the luminosity of those objects, in particular for close to Compton-thick AGNs

(e.g. NGC6240, Lutz et al. 2003). In order to help resolve these problems we have performed a mid-infrared spectroscopic study which is based on a large sample of infrared-faint and infrared-luminous LINERs. This study is the first of its kind, since only a few LINERs were observed with ISO as part of various projects with differing scientific goals (Satyapal, Sambuena, & Dudik 2004), resulting in a sparse collection of mid-IR LINER line detections of rather low S/N in a heterogenous sample. Comprehensive mid-infrared spectroscopic studies of LINERs have become possible only now with *Spitzer*.

2. Sample Selection, Observations and data Processing

We have based our selection of LINERs on the infrared luminosity of low redshift objects. Most of the IR-faint LINERs ($L_{IR}/L_B \lesssim 1$, with L_{IR} , the 8-1000 μ m luminosity, defined as in Sanders & Mirabel 1996) studied in the literature have compact nuclei (e.g. Pogge et al. 2000), consistent with photoionization from a central source. This central source is very likely an AGN, since most of these IR-faint LINERs have compact nuclear X-ray sources, but no extended X-ray sources (e.g. Carrillo et al. 1999, Satyapal et al. 2004). On the other hand, IR-luminous LINERs ($L_{IR}/L_B \gtrsim 1$) often also show compact hard X-ray cores indicative of an AGN, but in addition they often contain multiple off-nuclear X-ray point sources. There is evidence for extended LINER emission in a number of LINERs in the Revised Bright Galaxy Sample (RBGS, see Veilleux et al. 1995). A famous example is the extended LINER emission in NGC 6240 (Veilleux et al. 2003). Monreal-Ibero et al. (2006) also show IFU [NII]/H α excitation maps of IR-luminous LINERs showing extended LINER emission. Our two sub-samples of different IR-luminosity therefore represent statistically different LINER populations (nuclear versus extended LINER emission).

The sample is summarized in Table 1. We selected 16 IR-luminous LINERs from the RBGS, and 17 IR-faint LINERs from Ho et al. (1997). The IR-faint LINERs are further subdivided into 5 Type 1 and 6 Type 2 LINERs, and in addition 6 “transition” objects (see Ho et al. 1997, and §3.1). The infrared-bright LINERs are all of Type 2. With a median L_{IR} of 11.31 L_\odot the IR-luminous LINERs are much more luminous than the IR-faint LINERs in the IR, and there is no significant difference between the IR-faint sub-classes (L1: 8.92 L_\odot , L2: 9.27 L_\odot , T2: 9.31 L_\odot). For further multi-wavelength information for all our objects we refer to Carillo et al. (1999). Table 1 also lists L_{IR}/L_B ratios. The median ratios are 106 and 1.8 for the IR-bright and IR-faint LINERs respectively. The data were obtained with the InfraRed Spectrograph (IRS; Houck et al. 2004) on board *Spitzer* in staring mode. High resolution spectra covering 10 – 37 μ m (modules SH and LH) are complemented by low-resolution spectra in the 5 – 15 μ m range (modules SL2 and SL1). Our data reduction

process started with the two dimensional BCD products from the Spitzer pipeline (version S12). We used our own IDL routines to perform de-glitching, and SMART (Higdon et al. 2004) for the final spectrum extraction.

All our targets are nearby ($D \leq 120\text{Mpc}$), but on average the IR-faint LINERs have lower redshifts (median $z=0.004$) than the IR-bright objects (median $z=0.023$). We carefully checked that aperture effects (extended objects at different distances, and fluxes from different aperture sizes in the different IRS modules) do not significantly affect the spectra and our conclusions. For most of the targets the 12 and 25 μm flux densities agree quite well with the IRAS values (the worst deviation is a factor 2 in NGC5371, a nearby, IR-faint LINER which is dominated by mid-IR emission from the spiral arms); flux density discrepancies in the overlapping wavelength region between sub-spectra obtained with different aperture sizes are of the same order; and the profiles of most of the two-dimensional spectral images do not deviate significantly from stellar (point source) profiles. I.e. the observed flux in most of the objects is coming from a nuclear region of 0.3 kpc (median) diameter. We did not apply an extended source correction to the flux calibration, and we used full width apertures for the spectral extraction. More details about the sample, the observations and the data processing will be described in a forthcoming paper (D. Rupke et al., in prep.).

3. Mid-infrared properties of LINERs

Our new *Spitzer* observations provide three ways to distinguish among the various sub-classes of LINERs: the mid-infrared SEDs, the PAH emission features, and various combinations of IR fine-structure line ratios. These are illustrated and discussed below. Figure 1 shows the average spectra of both sub-samples (with the IR-faint LINERs further divided into the three subgroups Type 1, Type 2, and transition objects, see §2). As described in §2 the IR-faint LINERs, including the transition objects, are much less luminous in the IR than the IR-luminous ones. Before averaging, the individual spectra have been normalized at 19 μm . The average spectra show clear differences among the sub-groups. Because of a low dispersion within the two major groups (IR-luminous, IR-faint) almost all of our individual spectra can be unambiguously assigned to one of these two groups (Figure 2).

3.1. SED shape

The mid-infrared SEDs of IR-faint LINERs are clearly flatter (i.e., bluer) than their IR-luminous counterparts. No strong absorption features due to silicates (at 9.7 and 18 μm)

or ices (at various wavelengths) are seen in either sub-sample. Only one IR-faint LINER, NGC 3998, reveals strong silicate emission (Sturm et al. 2005). In contrast, the mid-infrared SEDs of infrared bright LINERs generally look very similar to those of starburst galaxies (e.g., Sturm et al. 2000). There are interesting trends in Figure 1. The Type 1 and Type 2 spectra are very similar, but below $\sim 15\mu\text{m}$ the average Type 1 spectrum has an additional warm (dust) component. The average Transition LINER lies in between the Type 1/Type 2 objects and the IR-bright LINERs. These transition objects are classified as objects with [O I] strengths intermediate between those of H II nuclei and LINERs, which could be explained either by a dilution of “true” LINER spectra with circumnuclear star formation or by stellar photoionization (see Ho et al. 1997).

The differences in the mid-IR SEDs of the two major LINER types are quantified in Figure 2 (left panel): in a diagram of the continuum flux ratios $f_\nu(15\mu\text{m})/f_\nu(6\mu\text{m})$ vs. $f_\nu(30\mu\text{m})/f_\nu(6\mu\text{m})$ IR-faint and IR-bright galaxies are nicely separated. The warmer spectrum of (some of) the Type 1 LINERs compared to the Type 2 LINERs (see also Fig. 1) could be the signature of a warm AGN continuum (as expected in a comparison of Type 1 and Type 2 AGNs, assuming the AGN unification model holds for LINERs). Maoz et al. (2005) have found a similar trend in the UV continuum of IR-faint LINERs. In addition, in some of the weaker, nearby IR-faint LINERS photospheric emission from old stellar populations in the center of the host galaxies may contribute significantly to the measured continuum in the range 5 to $\sim 8\mu\text{m}$. Using the same scaling factor as Lutz et al. (2004) to extrapolate from K-band to mid-IR, and assuming that most of the K-band flux in our IRS aperture is stellar, we conclude that this might indeed be the case for some of the IR-faint LINERs. Stellar contribution is probably not the sole explanation, however, because it could hardly explain the difference between (the average) Type 1 and Type 2 LINERs (the K-band/15 μm ratios are similar in both types), and because the typical signature of such a component, a decreasing continuum in the 5–8 μm range, is not prominent in most of the individual spectra.

3.2. PAH ratios

Figure 1 also shows significant differences in the PAH features in the spectra of the two LINER groups. In IR-bright LINERs the PAH spectrum is very similar to starburst galaxies. IR-faint LINERs have very weak PAH features in the 5–10 μm range, but a strikingly strong 11.2 μm feature. We note that, in principle, a higher degree of dilution by an additional warm dust component in the IR faint LINERs could cause errors in the flux measurements of PAHs in the 5–10 μm range, if the continuum has structure of similar width as the PAHs. For instance, strong silicate emission or absorption around 10 μm , if not

accounted for, could lead to systematically false flux values of broad PAH features like the 7.7/8.6 μm PAH complex. Such an effect, however, should not play a significant role in our measurements of the relatively narrow, well defined PAHs at 6.2, 11.2 and 12.7 μm . Based on the flux ratios of these PAH features at 6.2, 11.2, and 12.7 μm , we present in Figure 2 (middle panel) another diagnostic diagram for the distinction between IR-bright and IR-faint LINERs. Hony et al. (2001, their Figure 5) have constructed such a diagram using ISO spectra of galactic HII regions, YSOs and evolved stars/reflection nebulae. They found that the strongest 11.2 μm PAH features (lowest 12.7/11.2 and 6.2/11.2 ratios) are produced in evolved stars, while HII regions have the highest 12.7/11.2 (and 6.2/11.2) ratios. They attributed this to a different degree of ionization (the 11.2 μm PAH carriers are neutral, those of the 6.2 and 12.7 features are ionized; see also Joblin et al. 1996), as well as a processing of PAHs from large (11.2 μm) to smaller (12.7 μm) carriers. This could imply a less ionizing environment in the IR-faint LINERs than in the IR-bright ones, or significant differences in PAH formation and destruction.

3.3. Emission line ratios

The mid-infrared LINER spectra are rich in fine structure emission lines. We have detected strong [O IV] lines, i.e. highly ionized gas, in both LINER sub-samples, suggestive of the presence of an AGN in $\sim 90\%$ of the LINERs. The presence of a weak AGN in many of the IR-luminous LINERs is consistent with the compact hard X-ray cores that many IR-bright LINERs show (see §2), and is further supported by the detection of [Ne V] in about half of these sources. This detection rate is certainly a lower limit due to the limited S/N in the [Ne V] spectra. In order to explore differences in relative line strengths and physical properties, we have constructed mid-infrared diagnostic diagrams involving various combinations of these fine structure emission lines. The right panel in Figure 2 is an example of such a diagram using the line ratios of [Fe II]26.0 μm /[O IV]25.9 μm and [O IV]25.9 μm /[Ne II]12.8 μm . Lutz et al. (2003) used this diagram to distinguish among excitation by early type stars, AGNs, and shocks. Starburst galaxies, Seyfert galaxies, and supernova remnants (SNRs) are clearly separated in this line ratio plane. Interestingly, IR-luminous and IR-faint LINERs are easily distinguishable in this diagram: the IR-luminous LINERs all lie on a linear relation connecting starbursts and Seyferts, which might be explained by a minor AGN contribution in addition to the star forming regions (see mixing lines in Lutz et al. 2003). The position of the IR-luminous LINERs in this diagram is an indication, that the weak AGN in these objects is more Seyfert-like, i.e. not responsible for the IR-faint LINER emission. Surprisingly, the IR-faint LINERs are clearly off this line and lie in a region populated by SNRs. The reason for the differences between the two classes (and between IR-faint LINERS

and Seyferts) is so far uncertain. The role of the hardness of the radiation spectrum and of the ionization parameter, as well as the influence of shocks in both LINER classes has to be further examined. Can, e.g., photoionized spectra for certain hardness and ionization parameters reach the ‘SNR’ region in Figure 2c?

4. Conclusions and Outlook

Our systematic study of LINERs with *Spitzer* confirms that IR-luminous sources of this group are very different in their properties from IR-faint LINERs. IR-luminous LINERs have infrared SEDs that are similar to those of starburst galaxies, and they are situated in different regions of several diagnostic diagrams than IR-faint LINERs. While this has been suspected from previous multi-wavelength studies, the new mid-IR data provide the cleanest way to separate those groups. Many of these differences are also visible at low spectral resolution, and thus at high redshift, making our discovery an important cosmological tool for discerning the role of AGN in galaxy formation and evolution. A more detailed investigation of this issue and a quantification of the relative contributions from AGN and star formation to the LINER spectra requires a careful disentangling of the spectra into the various components (stellar, HII region, AGN, etc.), involving template fitting methods. Furthermore, for an understanding of the emission line properties, detailed photoionization modeling is required. This is the subject of a forthcoming paper (D. Rupke et al., in preparation).

This work is based on observations made with the Spitzer Space Telescope, which is operated by the Jet Propulsion Laboratory, California Institute of Technology under a contract with NASA. Support for this work was provided by NASA through an award issued by JPL/Caltech. AS and HN thank the Israel Science Foundation for support grants 221/03 and 232/03. HN acknowledges support by the Humboldt Foundation and thanks the host institution MPE.

References

Barth, A.J. & Shields, J.C. 2000, PASP, 112, 753
Brandl, B. et al., 2004, ApJS, 154, 188
Bressan et al. 1998, A&A, 332, 135
Bressan et al. 2006, ApJ, 639, L55
Carrillo, R., et al. 1999, RMxAA, 35, 187
Dopita, M. A., & Sutherland, R. S. 1995, ApJ, 455, 468
Ferland, G. J., & Netzer, H. 1983, ApJ, 264, 105
Groves et al. 2004, ApJS, 153, 9
Heckman. T.M. 1980, A&A, 87, 152
Ho, L.C., et al. 1997, ApJS, 112, 315
Hony, S., et al. 2001, A&A, 370, 1030
Higdon, S. J. U., et al. 2004, PASP, 116, 975
Houck, J. R., et al. 2004, ApJS, 154, 18
Joblin C., Tielens A.G.G.M., Geballe T.R., Wooden D.H. 1996, ApJ, 460, L119
Kewley, L. J. et al. 2006, astro-ph/0605681
Lutz, D., et al. 2003,A&A, 409, 867
Lutz, D., et al. 2004,A&A, 418, 465
Maoz, D. et al. 1998, AJ, 116, 55
Maoz, D., Nagar, N. M., Falcke, H., & Wilson, A. S. 2005, ApJ, 625, 699
Monreal-Ibero, A., Arribas, S., & Colina, L. 2006, ApJ, 637, 138
Monreal-Ibero, A., Arribas, S., & Colina, L. 2006, astro-ph/0509681
Pérez-González, P. G., et al. 2005, ApJ, 630, 82
Pogge, R. W. et al. 2000, ApJ, 532, 323
Quataert, E. 2001, ASP Conf. Proc., 224, p.71
Sanders, D. B., & Mirabel, I. F. 1996, ARA&A, 34, 749
Satyapal, S., Sambruna, R. M., & Dudik, R. P. 2004, A&A, 414, 825
Shull, J. M., & McKee, C. F. 1979, ApJ, 227, 131
Sturm, E., et al. 2000, A&A, 358, 481
Sturm, E., et al. 2005, A&A, 629, L21
Veilleux, S., et al. 1995, ApJS 98, 171
Veilleux, S. & Osterbrock, 1987, ApJS, 63, 295
Verma, A., et al. 2003, A&A, 403, 829

Table 1. The LINER Sample

Object Name	Catalog	Type	L_{IR}^a	L_{IR}/L_B^b	Object Name	Catalog	Type	L_{IR}^a	L_{IR}/L_B^b
UGC556	RBGS ^c	L2	10.91	106	NGC404	Ho97 ^d	L2	7.83	1.1
UGC2238	RBGS	L2	11.35	93	NGC3245	Ho97	T2	9.48	1.8
IRAS02438+2122	RBGS	L2	11.20	205	NGC3507	Ho97	L2	-	-
NGC1204	RBGS	L2	10.96	113	NGC3642	Ho97	L1	9.65	1.4
IRAS05187-1017	RBGS	L2	11.31	229	NGC3884	Ho97	L1	-	-
NGC4666	RBGS	L2	10.44	29	NGC3898	Ho97	T2	9.13	0.6
NGC4922	RBGS	L2	11.31	103	NGC3998	Ho97	L1	8.66	0.6
UGC8387	RBGS	L2	11.65	135	NGC4036	Ho97	L1	9.18	0.5
NGC5104	RBGS	L2	11.19	79	NGC4192	Ho97	T2	9.72	4.7
NGC5218	RBGS	L2	10.64	21	NGC4278	Ho97	L1	8.50	0.5
IZw107	RBGS	L2	11.89	-	NGC4419	Ho97	T2	9.91	11
IRAS15335-0513	RBGS	L2	11.42	-	NGC4435	Ho97	T2/H	9.09	1.9
IRAS16164-0746	RBGS	L2	11.44	210	NGC4457	Ho97	L2	9.27	4.3
ESO602-G025	RBGS	L2	11.33	47	NGC4486	Ho97	L2	8.95	0.1
Zw453.062	RBGS	L2	11.38	116	NGC5371	Ho97	L2	10.59 ^e	4.9
NGC7591	RBGS	L2	11.12	47	NGC6500	Ho97	L2	9.74	3.0
					NGC7177	Ho97	T2	-	-

^alogarithm of the 8-1000 μ m luminosity in units of the solar luminosity

^b B from B magnitudes in Carillo et al. (1999)

^cRBGS= Revised Bright Galaxy Survey, Veilleux et al. (1995)

^dHo97=Ho et al. (1997)

^enuclear LINER from Ho97, with much of the mid-IR luminosity coming from spiral arms outside the IRS apertures, hence treated as IR-faint LINER

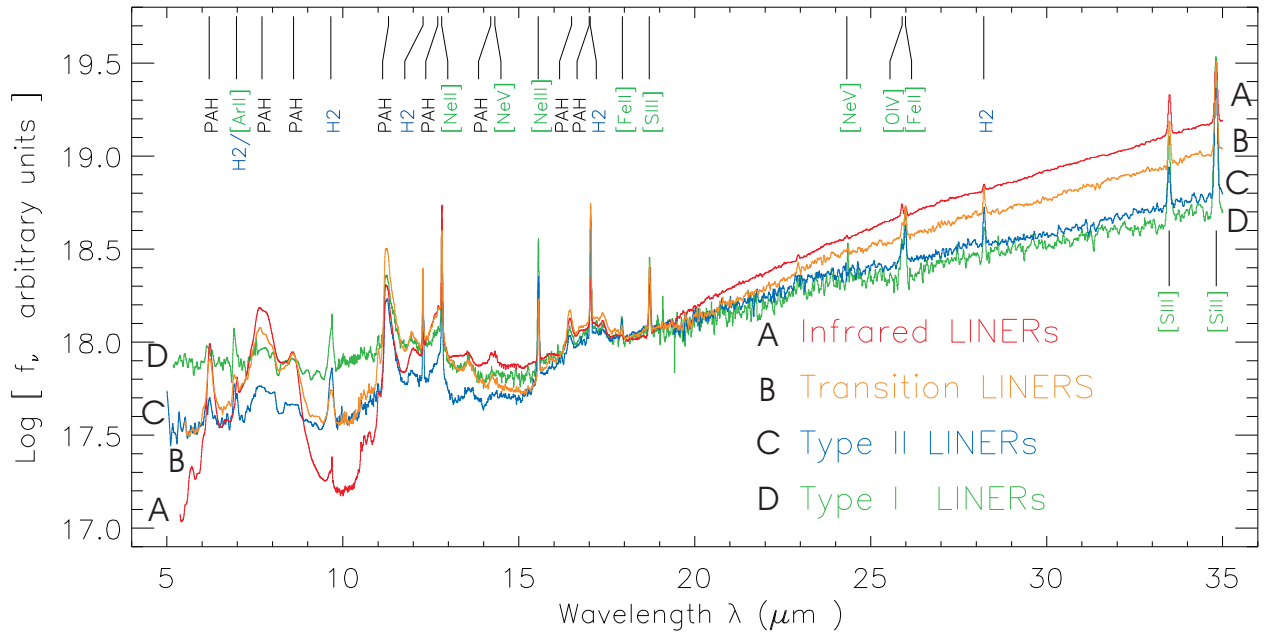


Fig. 1.— Composite spectra (normalized at $19\mu\text{m}$) of the 16 IR-luminous LINERs (red) and the IR-faint LINERs (green: 5 Type 1 LINERs, blue: 6 Type 2 LINERs, yellow: 6 Transition Type).

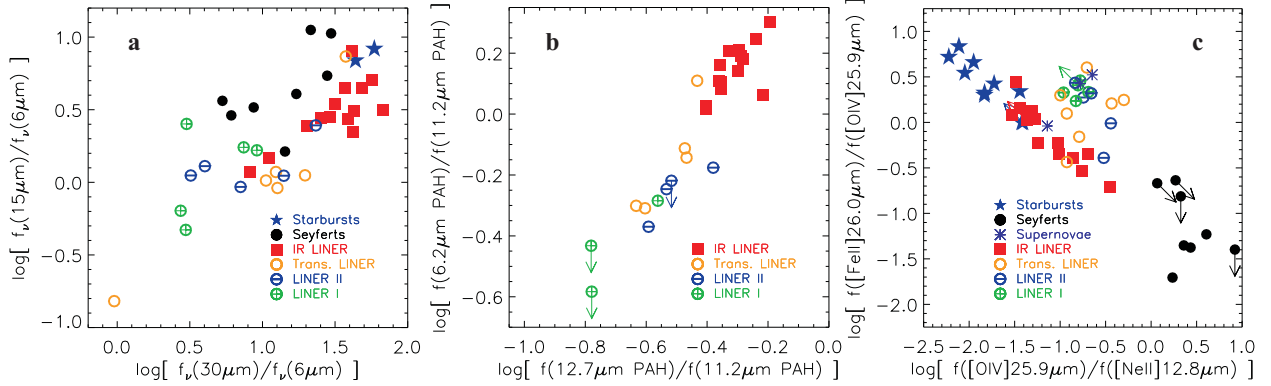


Fig. 2.— Mid-infrared diagnostic diagrams to distinguish between IR-luminous and IR-faint LINERs. In panel *a* Seyfert data are from Weedman et al. (2005), Starbursts from Sturm et al. (2000, M82) and Brandl et al. (2004, NGC7714); Starburst and Seyfert data in panel *c* are from Sturm et al. (2002) and Verma et al. (2003). Error bars in all three panels are comparable to the symbol sizes.